SNOWMELT DETECTION FROM SENTINEL-1 SYNTHETIC APERTURE RADAR IN THE LAJOIE BASIN, BRITISH COLUMBIA

Sara Darychuk[1], Joseph Shea [1], Anna Chesnokova[1], Brian Menounos[1], Frank Weber[2], and Georg Jost[2]

ABSTRACT

Snowmelt runoff supplements streamflow and soil moisture during warm summer months in Western North America. As direct snowpack measurements are sparse, many models exist to predict the release of runoff in alpine regions. An increase in spatially distributed observational data of seasonal snow may help to refine and improve these efforts going forward. Synthetic Aperture Radar (SAR) is sensitive to the liquid water content of snow and has been successfully used to map wet snow in alpine regions. We employ SAR and multispectral data to estimate the onset and duration of snowmelt in 2018 in the Lajoie Basin, British Columbia. We collate and process Sentinel-1, Sentinel-2 and Landsat-8 images in Google Earth Engine. A backscatter threshold is used to define the inferred period at which the snowpack is saturated and begins to generate runoff. Multispectral imagery is used to estimate snow-free dates across the basin to define the end of the snowmelt period. These methods are most effective on moderate to low slopes (< 30°) in open areas. This approach has high potential for adaptability to other alpine basins or regions and can be used for future model calibration. (KEYWORDS: snowmelt, snowpack dynamics, Synthetic Aperture Radar, remote sensing, Google Earth Engine)

INTRODUCTION

Runoff from snowmelt forms a vital part of the Earth's hydrological cycle and accounts for approximately 32% of global freshwater discharge (Meybeck et al., 2001). Current warming trends indicate snow cover may disappear earlier in the spring in future years, which has the potential to decrease aquatic ecosystem health and limit freshwater availability in the summer months (Barnett et al., 2005). Streamflow records are often used to infer changes in the timing of snowmelt runoff (Déry et al., 2009; Stewart, 2009; Stewart et al., 2004), and earlier spring snowmelt and decreased summer flows have been detected in glacial and nival watersheds across Western Canada between 1960 and 2006. While streamflow is a good proxy for inferring changes in snowmelt runoff regimes, it cannot be applied to ungauged basins.

Remote sensing data offer alternative methods to monitor snowmelt and estimate the timing of runoff from the snowpack (Marin et al., 2020). Synthetic Aperture Radar (SAR) is sensitive to the liquid water content of a snowpack and is often used to map wet snow via a simple algorithm known as Nagler's Method (Nagler & Rott, 2000; Rott & Nagler, 1994). With the launch of Sentinel-1 from the European Space Agency in 2014, SAR became a more viable option for snow monitoring as data is available at six-day intervals with a 10 m pixel resolution. Marin et al. (2020) demonstrated the sensitivity of Sentinel-1 SAR to snow water equivalence (SWE) and snowpack liquid water content (LWC) at five test sites in the European alps. From the SAR time series three melting phases within the snowpack were identified: moistening, ripening, and runoff (Marin et al., 2020). During runoff the snowpack is completely saturated as has begun to release liquid water (Marin et al., 2020).

Many watersheds in Western North America are extensive and have few physical observations in the form of snow pillows, snow courses, or stream gauges. SAR can provide the spatially distributed measurements needed to monitor snowmelt, as the minimum value in a SAR time series has been shown to correspond with the release of liquid water, or runoff, from the snowpack (Marin et al., 2020). In this paper we fuse C-band Sentinel-1 SAR imagery with Landsat-8 and Sentinel-2 multispectral imagery to define the onset and duration of snowmelt in the Lajoie Basin, a large watershed in the Southern Coast Mountains of British Columbia. Remote sensing data were analyzed and collated using Google Earth Engine (GEE), a cloud computing platform with access to a multi-petabyte catalog of analysis ready data (Gorelick et al., 2017).

Paper presented Western Snow Conference 2021
[1]University of Northern British Columbia, Prince George, B.C., V2N 4Z9
Corresponding Author: darychuk@unbc.ca
[2]BC Hydro, 6911 Southpoint Drive, Burnaby, B.C., V3N 4X8

METHODS

GEE was used to determine snowmelt onset dates from Sentinel-1 SAR images. For this analysis, snowmelt is considered the period of time when the snowpack is releasing liquid water or producing runoff. SAR scenes were filtered to create a collection of images containing the Lajoie Basin captured between February 2018 and September 2018. Temporal stacks for each directional pass of the satellite, ascending or descending, were created and corrected for slope-induced radiometric distortion using a volumetric model (Vollrath et al., 2020). The minimum backscatter value for each pixel was identified and the corresponding date was extracted. The minimum dates were taken to be the date of runoff onset from the snowpack (Marin et al., 2020) with the assumption that every pixel in the basin became snow covered. Finally, pixels were resampled to 30 m for fusion with optical data. These methods were performed for images captured in VV (Vertical-Vertical) and VH (Vertical-Horizontal) polarization. Snowmelt onset dates for both polarizations were then smoothed using a median circular moving window filter with a 60 m radius.

SAR time series were also extracted in GEE using the created Sentinel-1 temporal stacks. Land cover classes were created for bare ground, immature forest, mature forest, water, and ice in the study area. Slope classes of 10° were also created in GEE using a 5 m LiDAR digital elevation model. SAR time series were then averaged by land cover type and slope between elevations of 1600 m and 1800 m.

GEE was used to determine snow free dates from Sentinel-2 and Landsat-8 images. Sentinel-2 and Landsat-8 scenes were filtered to create a collection of images containing the Lajoie Basin captured between February 2018 and September 2018. Images were masked for clouds and fused into a single image collection. Normalized Difference Snow Index (NDSI) and Normalized Difference Forest Snow Index (NDFSI) values were calculated over non-glaciated areas of the basin to classify each image for snow cover using a threshold of 0.4 (Table 1). For glaciated areas of the Lajoie Basin the initial image collection was classified for snow cover using a K-means clustering algorithm. Two classes were created on the glacier, snow and ice, based on reflectance values in the visible, near infrared, and shortwave infrared spectrums. For all areas in the basin the first snow free date per pixel was selected and the corresponding date was extracted. Snow free dates were then smoothed using a median circular moving window filter with a 60 m radius.

Table 1. Indices used to detect snow cover in multispectral and optical imagery.

Index	Formula	Source
Normalized Difference Snow Index (NDSI)	$\frac{green - swir2}{green + swir2}$	(Hall et al., 1995)
Normalized Difference Forest Snow Index (NDFSI)	$\frac{nir - swir2}{nir + swir2}$	(Wang et al., 2015)

The duration of snowmelt was determined per pixel from the difference in days between SAR estimates of snowpack runoff onset and optical estimates of snow free dates. Estimates snowmelt duration were then analyzed for trends by aspect and elevation.

SAR estimates of snowmelt onset and duration were validated with continuous records of temperature and SWE from the Downton Lake Upper Automated Hydrometeorological Station (AHS) in the Lajoie Basin. Hourly SWE measurements were averaged per day and maximum SWE was calculated for the 2018 snow season. Snowmelt duration from AHS records was taken as the time between 95% maximum and 5% maximum SWE. Hourly temperature measurements were averaged for each day and evening in 2018. Snowmelt onset from temperature was taken to be the first occurrence of nighttime air temperatures exceeding 0 °C for at least three days.

RESULTS AND DISCUSSION

After investigating SAR time series over the study area it was determined that VH or cross-polarized images produced a smoother time series than VV or co-polarized images. Vegetation covers a significant proportion

of the total area of the Lajoie Basin, approximately 45%. Manickam & Barros (2020) found that backscatter coefficients from cross-polarization were more sensitive to snow cover below the tree line. Furthermore, the harsh terrain in the study area may amplify the observed noise in co-polarized images, agreeing with findings from Nagler et al. (2016). Steep slopes reduce the ability of VV polarization to distinguish between wet snow and snow free surfaces (Nagler et al., 2016). The combination of steep slopes and forested regions present in the Lajoie Basin make VH polarized images more suitable for watershed scale snowmelt mapping. As a result, the analysis was performed only on VH polarized images.

Snowmelt onset estimates derived from SAR agree with SWE and temperature records from snow pillow observations in the Lajoie Basin. In 2018 SAR minima from Sentinel-1 captured snowmelt onset within ± 6 days at the Downton Lake Upper AHS (Figure 1). A three-day threshold for sustained above 0°C nighttime air temperatures was found to be appropriate for this study area, as shorter periods identified snowmelt onset too early in the season (for example in 2018 there was a two-day exceedance in mid-January). Using a longer threshold period (i.e., 5 days or 7 days) had little impact on the estimated snowmelt onset date as the exceedances are substantial in the late spring and summer, lasting 139 days in 2018.

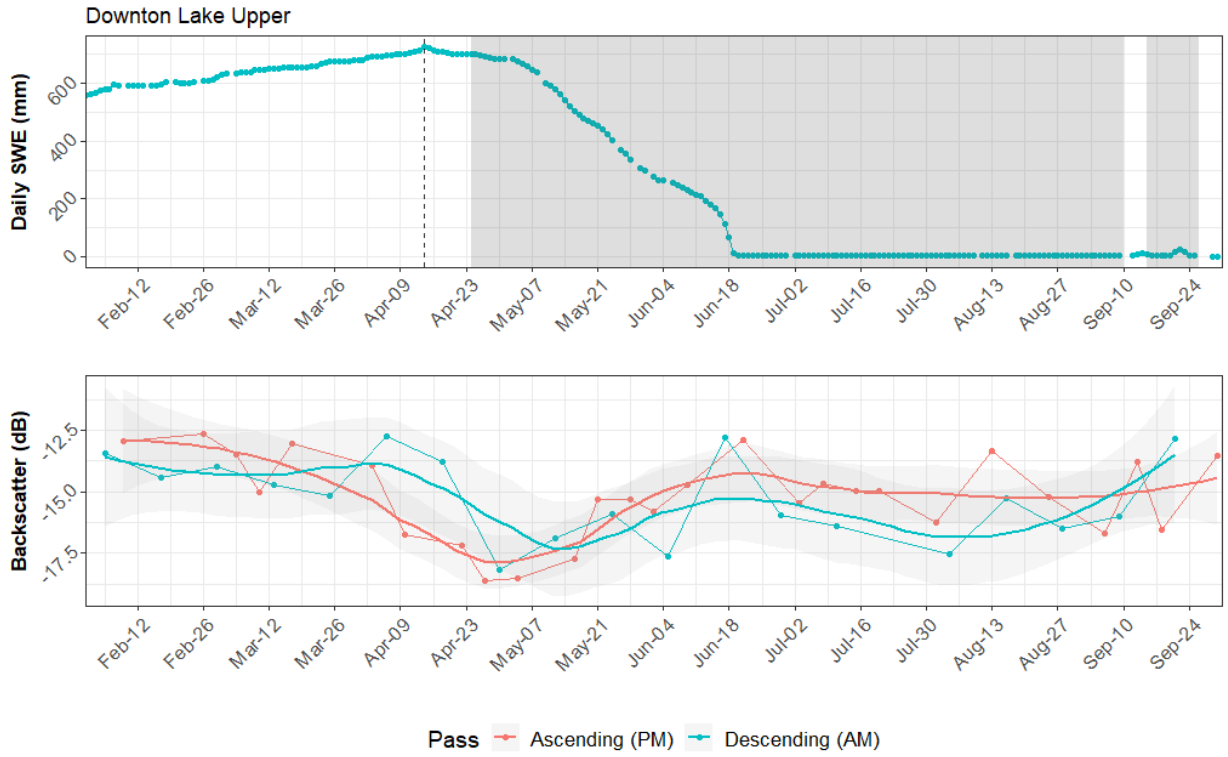

Figure 1. Snow water equivalence (SWE) and SAR backscatter signals at the Downton Lake Upper station in the Lajoie Basin, 2018. The top graph displays SWE records. The vertical dashed line represents the day of maximum SWE, whereas the shaded regions indicate periods of time when nighttime air temperatures were above 0 °C for at least three days. The first day of the nighttime air temperature exceedance period is taken as the onset of snowmelt which in 2018 was the 24th of April. The bottom graph displays average backscatter from Sentinel-1 SAR images. The marker for snowmelt onset is taken to be day when SAR values are at their minimum. In 2018 these dates were the 27th of April and the 30th of April for the ascending and descending passes, respectively.

Land cover type and slope had the largest impact on the effectiveness of SAR minima for detecting snowmelt onset. Clearly defined minima are visible in open areas, however, in mature forest they become less evident (Figure 2). While the co-polarized images allowed for snowmelt to be detected over the majority of vegetated surfaces, dense forest cover still increased noise in the signal. Backscatter values were higher under mature forest cover in the study area (Figure 2). A variety of factors, such as snowpack structure and forest stem

volume, may contribute to this. The correlation between stem volume and backscatter values varies in sign and magnitude depending on the composition of the forest and local climate (Santoro et al., 2019).

Slope also had a large impact on the ability of cross-polarized SAR images to capture snowmelt onset. The 'U' shape of the backscatter time series is most pronounced on gentle slopes (<10°) and becomes harder to detect as slope increases (Figure 2). Manickam & Barros (2020) had similar findings in the Swiss Alps, where between April and May backscattering coefficients were less sensitive to wet snow as slope increased.

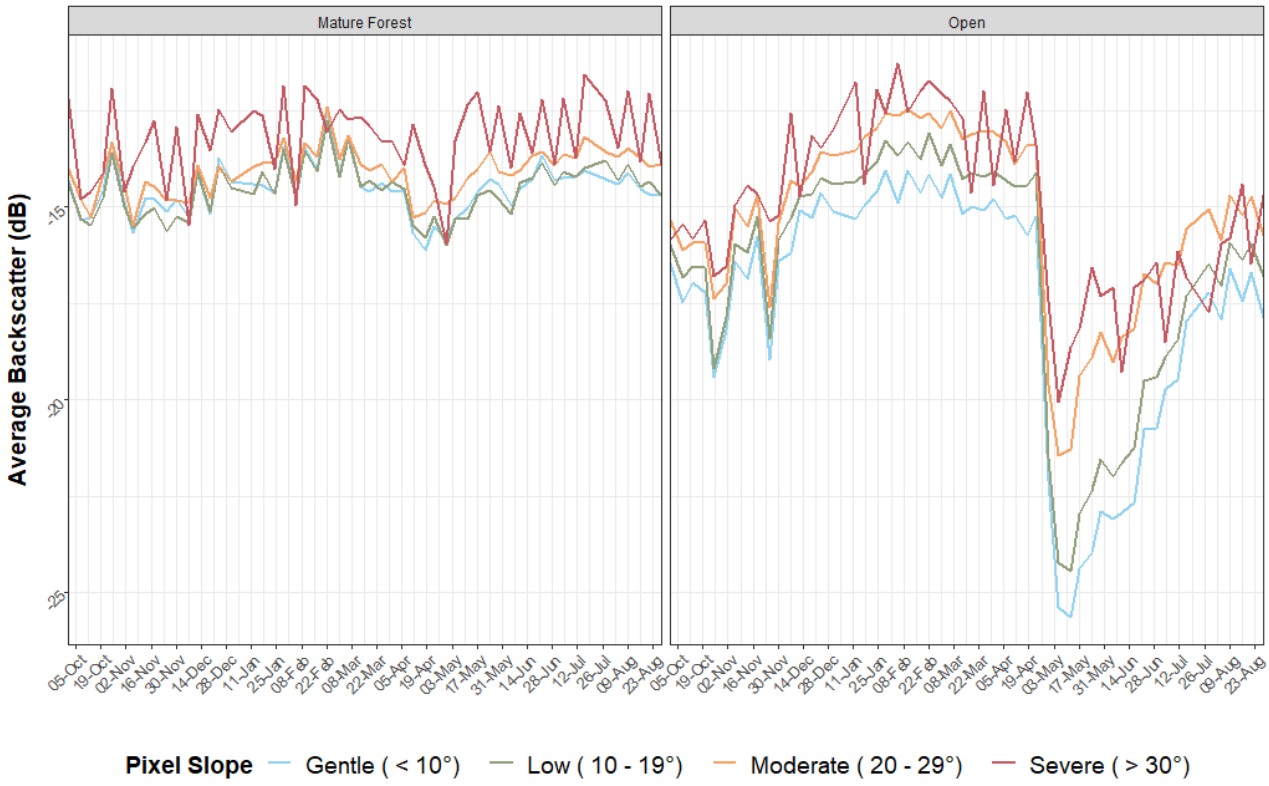

Figure 2. SAR backscatter time series in the Lajoie Basin for the 2018 snow season. Observations under mature forest cover are displayed on the left, whereas observations in open areas are displayed on the right. Average backscatter for each cover type is shown by the shaded lines, with each line representing a different slope category. Observations are from pixels located between 1600 m and 1800 m.

Snow-free dates from Landsat-8 and Sentinel-2 images were the most consistent in open areas. While the use of NDFSI improved the detection of snow disappearance under mature forest cover, ablation in these regions still appeared patchier than expected (Figure 3). Clouds were an additional barrier for snow detection from optical and multispectral data. Cloud cover is persistent at high elevations during the ablation season in the Lajoie Basin. Missing data from cloud cover reduces the temporal resolution at which imagery is available, decreasing the accuracy of snow disappearance estimates.

SAR snowmelt duration estimates formed consistent patterns based on aspect and elevation, with exceptions occurring on steep slopes and in densely forested regions. (Figure 3). Snowmelt durations were the longest on northern and eastern facing slopes at elevations between 2000 m and 2200 m. The observed trends in snowmelt durations agree with trends in snow depths observed in the study area. The snowpack is generally deepest at mid to high elevations in the Lajoie Basin, as at the highest elevations there is heavy redistribution of snow by wind and avalanching. At Downton Lake Upper snowmelt duration was 46 days from SWE records. At the same location snowmelt duration was estimated to be 41 days from data fusion products. While snowmelt duration estimates from data fusion agree with SWE records at the Downton Lake Upper AHS, additional field measurements are required to assess the accuracy of these methods at the watershed scale.

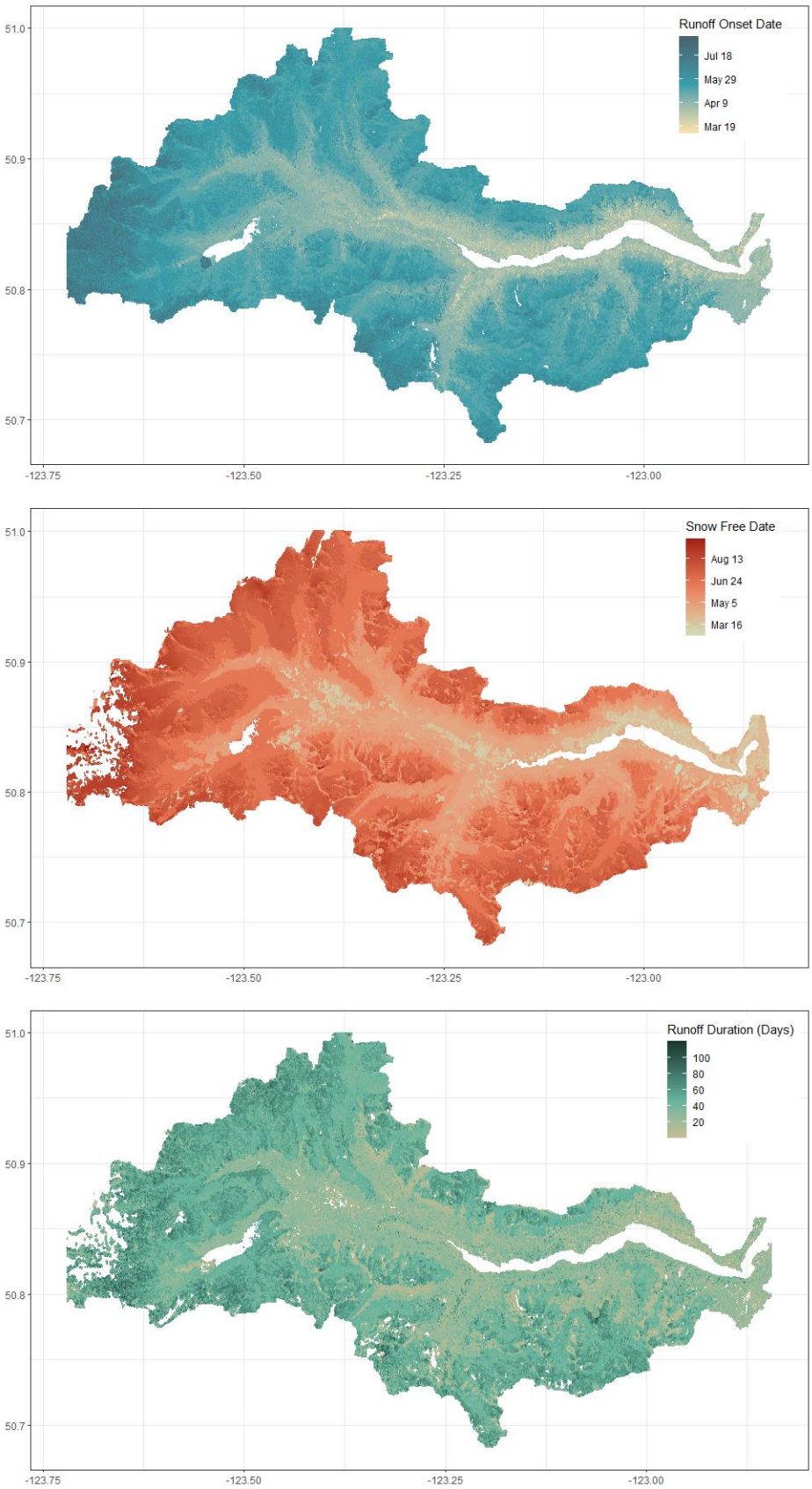

Figure 3. Snowmelt onset, snow free dates and snowmelt duration maps for 2018 in the Lajoie Basin. The top map depicts snowmelt runoff onset from Sentinel-1 SAR. The middle map depicts snow free dates from Sentinel-2 and Landsat-8 multispectral and optical data. The bottom map depicts snowmelt runoff duration in the Lajoie Basin from the created snowmelt onset and snow free date maps.

CONCLUSIONS AND OUTLOOK

The created image fusion products can provide estimates of snowmelt onset and duration in ungauged basins to watershed managers. Through using GEE and open-source satellite data this method is low cost and easily adaptable to other regions. In North America, runoff from melting snow forms a large component of available freshwater, performing key ecosystem functions and providing indications of climate change on a watershed level (Stewart et al., 2004). Sentinel-1 SAR can be used to monitor snowmelt patterns so we can better understand and anticipate changes to this valuable resource.

Future work explores the impact of stem volume on backscatter signals in regions with mature forest cover. However, the methods presented in this paper will require significant adaptation to address this. C-Band SAR is less sensitive to forest cover (when compared to L-Band SAR) and may not be suited for snowpack analysis in densely forested areas (Kumar et al., 2019; Santoro et al., 2019). Additional research will examine interannual variability in snowmelt onset and duration between 2018 and 2020 in the Lajoie Basin. Investigations will be made into the influence of temperature and precipitation on the observed patterns of snowmelt between study years. To validate the utility of SAR for snowmelt monitoring, field observations of snowpack LWC will be provided for the 2022 snow season.

REFERENCES

Barnett, T. P., Adam, J. C., & Lettenmaier, D. P. 2005. Potential impacts of a warming climate on water availability in snow-dominated regions. *Nature*, 438(7066), 303–309.

Déry, S. J., Stahl, K., Moore, R. D., Whitfield, P. H., Menounos, B., & Burford, J. E. 2009. Detection of runoff timing changes in pluvial, nival, and glacial rivers of western Canada: western Canada runoff timing. *Water Resources Research*, 45(4). https://doi.org/10.1029/2008wr006975

Gorelick, N., M. Hancher, M. Dixon, S. Ilyuschenko, D. Thau, & Moore R. 2017. Google Earth Engine: Planetary-scale geospatial analysis for everyone. *Remote Sensing of Environment* 202(1), 18-27.

Hall, D. K., Riggs, G. A., & Salomonson, V. V. 1995. Development of methods for mapping global snow cover using moderate resolution imaging spectroradiometer data. *Remote Sensing of Environment* 54(2), 127–140. https://doi.org/10.1016/0034-4257(95)00137-p

Kumar, A., B S P, Saikia, P., Deka, J., Bharali, S., Singha, L. B., Tripathi, O. P., & Khan, M. L. 2019. Tree diversity assessment and above ground forests biomass estimation using SAR remote sensing: A case study of higher altitude vegetation of North-East Himalayas, India. *Physics and Chemistry of the Earth*, 111, 53–64. https://doi.org/10.1016/j.pce.2019.03.007

Manickam, S., & Barros, A. 2020. Parsing Synthetic Aperture Radar Measurements of Snow in Complex Terrain: Scaling Behaviour and Sensitivity to Snow Wetness and Landcover. *Remote Sensing*, 12(3), 483.

Marin, C., Bertoldi, G., Premier, V., Callegari, M., Brida, C., Hürkamp, K., Tschiersch, J., Zebisch, M., & Notarnicola, C. 2020. Use of Sentinel-1 radar observations to evaluate snowmelt dynamics in alpine regions. *The Cryosphere*, 14(3), 935–956.

Meybeck, M., Green, P., & Vörösmarty, C. 2001. A New Typology for Mountains and Other Relief Classes. *Mountain Research and Development*, 21(1), 34–45.

Nagler, T., & Rott, H. 2000. Retrieval of wet snow by means of multitemporal SAR data. *IEEE Transactions on Geoscience and Remote Sensing*, 38(2), 754–765.

Nagler, T., Rott, H., Ripper, E., Bippus, G., & Hetzenecker, M. 2016. Advancements for Snowmelt Monitoring by Means of Sentinel-1 SAR. *Remote Sensing*, 8(4), 348.

Rott, H., & Nagler, T. 1994. Capabilities of ERS-1 SAR for snow and glacier monitoring in alpine areas. *European Space Agency-Publications-ESA SP*, 361, 965–965.

Santoro, M., Cartus, O., Fransson, J. E. S., & Wegmüller, U. 2019. Complementarity of X-, C-, and L-band SAR Backscatter Observations to Retrieve Forest Stem Volume in Boreal Forest. *Remote Sensing* 11(13), p. 1563. https://doi.org/10.3390/rs11131563

Stewart, I. T. 2009. Changes in snowpack and snowmelt runoff for key mountain regions. *Hydrological Processes*, 23(1), 78–94.

Stewart, I. T., Cayan, D. R., & Dettinger, M. D. 2004. Changes in Snowmelt Runoff Timing in Western North America under a `Business as Usual' Climate Change Scenario. *Climatic Change* 62(1-3), 217–232. https://doi.org/10.1023/b:clim.0000013702.22656.e8

Vollrath, A., Mullissa, A., & Reiche, J. 2020. Angular-Based Radiometric Slope Correction for Sentinel-1 on Google Earth Engine. *Remote Sensing*, 12(11), 1867.

Wang, X.-Y., Wang, J., Jiang, Z.-Y., Li, H.-Y., & Hao, X.-H. 2015. An Effective Method for Snow-Cover Mapping of Dense Coniferous Forests in the Upper Heihe River Basin Using Landsat Operational Land Imager Data. *Remote Sensing* 7(12), 17246–17257. https://doi.org/10.3390/rs71215882